

The Whitehill Formation as a Potential Analogue to the Acid Mine Drainage Issues in the Witwatersrand, South Africa

Dikeledi Tryphina Mashishi¹, Christian Wolkersdorfer^{1,2}

¹*Tshwane University of Technology (TUT), Department of Environmental, Water & Earth Sciences, Private Bag X680, Pretoria, 0001, South Africa*

²*Lappeenranta University of Technology, Laboratory of Green Chemistry, Sammonkatu 12, 50130 Mikkeli, Finland, christian@wolkersdorfer.info*

Abstract Acid mine drainage issues have been a cause for worldwide concern. This study assessed the potential of the Whitehill Formation as an analogue to the acid mine drainage issues in the Witwatersrand, South Africa. Evaluation of the Whitehill Formation suggests that the outcrop of gypsum in the formation is derived from reaction of pyrite-bearing shale with calcite. In order to determine this, the geochemical, geological and palaeoclimatic setting and strata similar to the formation were investigated. In addition, chemical-thermodynamic modelling (PHREEQC) was used for simulations. The results of this study show that metals precipitated out of the rock-water solution to form various mineral phases.

Key words Acid mine drainage, Witwatersrand basin; natural analogue, Whitehill Formation; similar strata; geochemical modelling

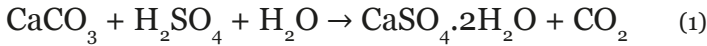
Introduction

Environmental effects associated with mining often affect the natural water environment, thus resulting in acid mine drainage generation (AMD) (Younger & Wolkersdorfer 2004). Acid mine drainage is formed by the oxidation of pyrite in the presence of oxygen and water (Stumm & Morgan 1996). In South Africa, the rocks of the Witwatersrand Basin consist primarily of 70–90% quartz and 3–5% pyrite and the main reefs are situated underneath a dolomitic karst aquifer (Durand 2012). Mining activities in the Witwatersrand Basin have been in place for over 100 years, with some of the pyrite deposited on tailing dumps, thus resulting in the generation of acidic mine waters which discharge approximately 14.17 m³/h of mine water (Masindi et al. 2016; McCarthy 2011).

In order to reconstruct the occurrence of natural processes of over millions (Ma) to billions (Ga) of years ago, this study uses a natural analogue, which has also been used elsewhere (Bruno et al. 2002). Throughout the entire Karoo Basin, the Whitehill Formation occurs and is overlain by the Collingham Formation and underlain by the Prince Albert Formation (Cole & Basson 1991). Deposition of the Whitehill Formation was about 275 Ma ago under deep marine anoxic conditions which prevailed until the deposition of the Collingham Formation. In addition, the Whitehill Formation is predominantly comprised of pyrite-bearing shale, black carbonaceous mudstone, organic rich matter, dolomite, quartz and gypsum outcrops (Smithard et al. 2015; Branch 2007). According to Geel et al. (2015), the pyrite-bearing shale close to contact with the Whitehill Formation is framboidal pyrite which is its most reactive form as described by Nordstrom (1982).

In a natural environment, sulfate deposits are exposed to water through joints and fissures in order to generate sulfate solutions. When in contact with carbonates, sulfate solutions react with

calcium to promote the precipitation of gypsum ($\text{CaSO}_4 \cdot 2\text{H}_2\text{O}$) as associated with the distribution of Ca^{2+} and SO_4^{2-} . This chemical process is given by the following equation (Lottermoser 2010):



Strata similar to the Whitehill Formation are the Marcellus Formation (United States of America), Irati Black Shale Formation (Uruguay), Mangrullo Formation (Argentina, Paraguay and Uruguay), Tacuary Formation (Paraguay), Barnett Shale Formation (United States of America), Kupferschiefer Shale Formation (Germany) and the Moenkopi Formation (United States of America) (Geel et al. 2015, Stewart et al. 1972). All strata similar to the Whitehill Formation describe the precipitation of gypsum which formed as a result of acid rock drainage (ARD). In this study, we determine whether gypsum of the Whitehill Formation is associated with ARD using geochemical modelling which comprises of the combination of field and laboratory experiments in order to understand current AMD issues.

Methods

A total of seven rock samples were collected from the outcrops of the Whitehill Formation in Loeriesfontein, Calvinia and Laingsburg, South Africa (table 1). In order to determine the major and trace metals of the samples, X-ray fluorescence was used (PANalytical Axios X-ray fluorescence spectrometer: Council of Geoscience). In TUT's mine water laboratory, batch tests with 400 mL of distilled water added to rock samples for analysis of the aqueous solution development were conducted. Furthermore, the parameters pH and electrical conductivity were determined over twelve weeks using Hach pHC201 and Hach CDC401 probes, connected to a Hach HQ40d. Also, at the end of the analysis, filtered samples were taken (0.45 μm nylon membrane syringe filters) and the residual water metal ion concentration were measured using inductively couple plasma-emission spectroscopy (9000 model ICP-OES at the Department of Chemical Engineering, in Tshwane University of Technology). In addition, ion chromatography (883 model: TUT Environmental and Analytical Chemistry Research laboratory) was used for anion analyses. Samples were measured in triplicate and results are reported as the mean. Results of the water quality parameters were verified by WaterLab. Moreover, results of aqueous solution were used in PHREEQC (WATEQ4F database) in order to calculate ion activities and saturation indices (SI) of mineral phases.

Principal component analysis (variance-covariance) was used to classify the seven samples (Past 3.15 from Øyvind Hammer).

Table 1 Geographical coordinates, WGS84

| Sample | Geodetic Datum |
|--------|--------------------------|
| LF1 | 30°56'52" S, 19°25'51" E |
| LF2 | 30°56'35" S, 19°25'59" E |
| CV | 31°29'20" S, 19°28'48" E |
| LB1 | 33°12'13" S, 20°37'41" E |
| LB2 | 33°10'58" S, 20°49'03" E |

Field Observations

In Loeriesfontein (LF1), an outcrop of a total length of approximately 100–150 m was investigated (figure 1). It is comprised predominantly of fresh brown shale interlayered with weathered shale which appears as a thin white band of gypsum (0–40 cm). In addition, it is overlain by fresh grey shale (40–63 cm), white gypsum interlayered with light yellow iron oxyhydroxides (60–63 cm), fresh grey brownish shale (63–88 cm), white gypsum interlayered with light yellow iron oxyhydroxides (88–94 cm) and fresh dark grey shale (94–140 cm). At Loeriesfontein LF2, approximately 400m south-west of LF1, the black shale (60%) was weathered to a distinctive white colour (40%) with very minor light yellow staining of Fe oxyhydroxides (figure 2).

Initially, batch test experiments were conducted for 54 days and later continued from day 127 until day 191, with a total of 12 weeks of analysis (figure 3). Changes in pH values occur either when sulfate solutions or carbonates are depleted. For instance, when the sulfate secondary minerals are depleted, the pH values will rise from acidic to circum-neutral values and alternatively, when carbonates are depleted, pH values will remain constant in circum-neutral pH values. In low pH waters the concentrations of Fe and SO_4^{2-} are high and indicate that pyrite oxidation occurs.

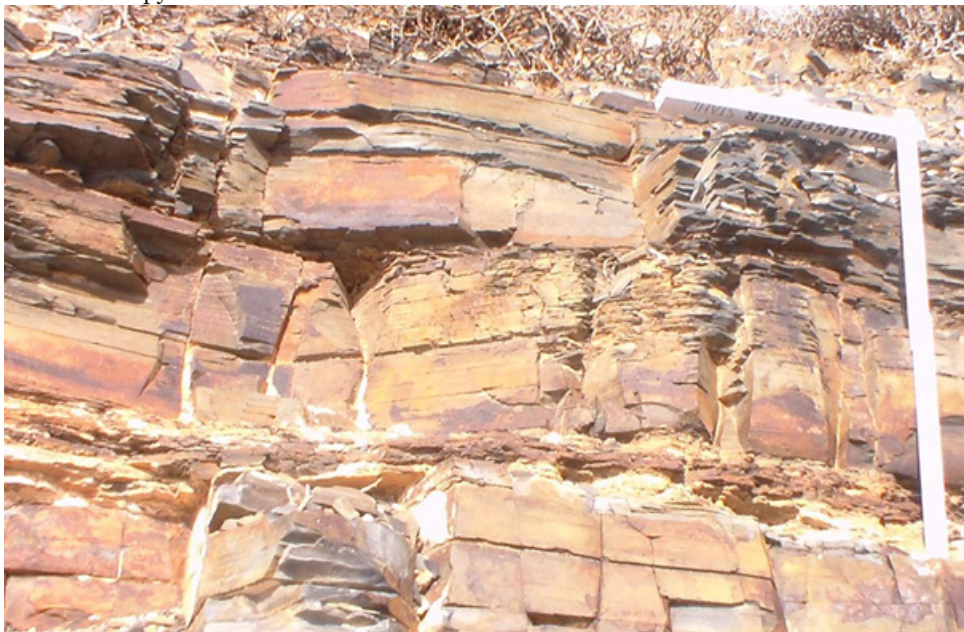


Figure 1 Fresh outcrop of the Whitehill Formation near Loeriesfontein (LF1).



Figure 2 Black shale weathered to a white colour near Loeriesfontein (LF2)

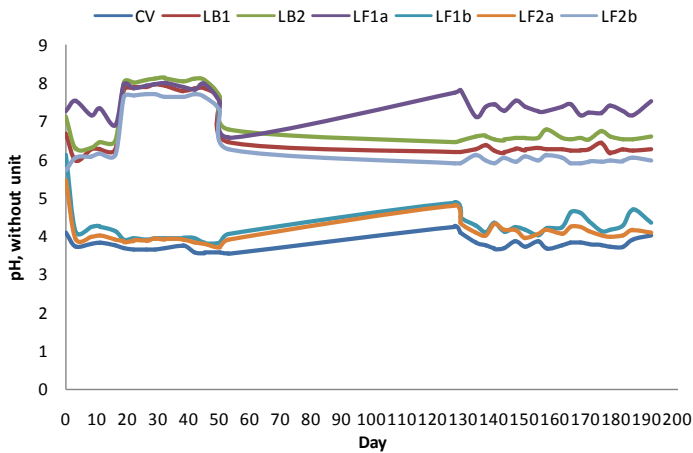


Figure 3 Batch test Laboratory pH results of the seven samples.

Results and Discussion

Major elemental analysis

A detailed database of major elements was used to identify the processes that occur in ARD environment. Results show the presence of CaO and MgO which correspond with the occurrence of carbonate rock. Moreover, high CaO and MgO contents in samples with acidic pH values and low content in samples with circum-neutral pH values were observed. An opposite trend to the CaO concentrations is observed for SiO₂, with high concentrations of SiO₂ in circum-neutral pH values and low concentrations in acidic pH values (table 2). SiO₂ corresponds with the occurrence of quartz/clay content which can also be used in the ratio to the Al₂O₃, to indicate changes in sedimentary conditions during deposition. In addition, the presence of pyrite and siderite can be indicated by elevated Fe₂O₃/K₂O ratios.

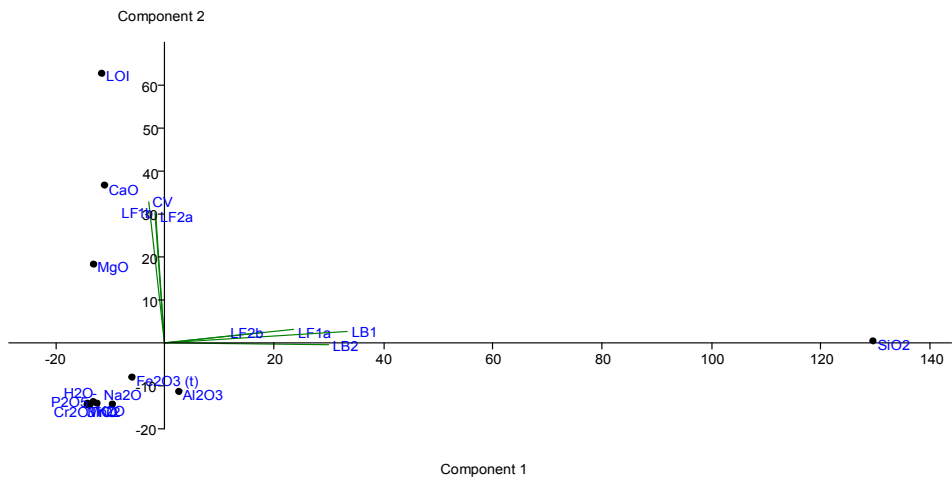


Figure 4 Scatter plot of principal component analysis results.

Table 2 Major elemental rock composition (%) of the seven samples.

X-ray Fluorescence Spectrometry (XRF); t: iron oxidized in the +3 state; LOI: loss of ignition; H₂O: moisture water.

| Parameter | LF1a | LF1b | LF2a | LF2b | CV | LB1 | LB2 |
|------------------------------------|--------|-------|--------|-------|--------|--------|--------|
| SiO ₂ | 63.89 | 3.79 | 4.04 | 50.30 | 1.31 | 88.93 | 79.64 |
| TiO ₂ | 0.51 | 0.04 | 0.05 | 0.81 | 0.02 | <0.01 | 0.12 |
| Al ₂ O ₃ | 13.77 | 1.02 | 1.43 | 14.47 | 0.59 | 0.44 | 10.40 |
| Fe ₂ O ₃ (t) | 4.76 | 4.28 | 5.32 | 10.96 | 0.27 | 3.40 | 1.21 |
| MnO | 0.004 | 0.164 | 0.173 | 0.178 | 0.048 | 0.014 | 0.069 |
| MgO | 0.59 | 18.06 | 16.60 | 9.00 | 21.34 | 0.22 | <0.01 |
| CaO | 0.25 | 28.74 | 29.27 | 10.21 | 29.87 | 3.62 | 1.46 |
| Na ₂ O | 1.67 | <0.01 | <0.01 | 2.12 | <0.01 | <0.01 | 5.80 |
| K ₂ O | 3.77 | 0.09 | 0.12 | 0.25 | 0.04 | 0.02 | 0.16 |
| P ₂ O ₅ | 0.085 | 0.28 | 0.14 | 0.14 | 0.207 | 0.04 | 0.08 |
| Cr ₂ O ₃ | 0.009 | 0.008 | 0.007 | 0.080 | 0.004 | 0.044 | 0.021 |
| LOI | 10.74 | 43.40 | 42.91 | 1.14 | 46.42 | 3.43 | 1.13 |
| Total | 100.05 | 99.88 | 100.06 | 99.66 | 100.12 | 100.16 | 100.09 |
| H ₂ O | 1.73 | 0.44 | 0.41 | 0.63 | 0.24 | 0.22 | 0.17 |

Performed by Council for Geosciences

Water quality parameters and pH analysis

Lab pH of the seven batch experiments ranged between 3.49 and 8.37 and the electrical conductivity (EC) between 73 and 7888 $\mu\text{S}/\text{cm}$. The results show that samples from LF1b, LF2a and CV developed low pH values and samples from LF1a, LF2b, LB1 and LB2 developed circum-neutral pH values, which can also be seen by the results of the principal component analysis (fig. 4). Initially, cations and anions were analysed to determine the concentration of elements in solution, which promote the results of batch experiments (table 3). In addition, results of aqueous solutions were used to predict potential precipitation of minerals in AMD environments. As a result, minerals which precipitate are carbonates, oxyhydroxide carbonates, metal oxides and oxyhydrosulfates as suggested by the presence of Al, Ca, Fe, Mg and Mn.

Table 3 Elements in mg/L, electrical conductivity (EC) in $\mu\text{S}/\text{cm}$, pH without unit.

| Parameter | LF1a | LF1b | LF2a | LF2b | CV | LB1 | LB2 |
|-------------------------------|-------|-------|-------|-------|-------|-------|-------|
| pH | 7.17 | 4.35 | 4.05 | 5.99 | 3.87 | 6.22 | 7.78 |
| EC | 477 | 2840 | 1338 | 1873 | 5570 | 139 | 132 |
| Al | <0.10 | 7.40 | 4.84 | <0.10 | 24.0 | <0.01 | 0.23 |
| B | <0.02 | <0.15 | 0.06 | <0.20 | 0.28 | <0.02 | <0.02 |
| Ca | 108 | 614 | 209 | 606 | 608 | 23 | 39.0 |
| Fe | <0.03 | 0.03 | <0.03 | <0.03 | 0.04 | <0.03 | <0.03 |
| K | 38.0 | 29.0 | 23.0 | 18.0 | 41.0 | 2.4 | 5.60 |
| Li | <0.01 | 0.09 | <0.03 | 0.04 | 0.24 | <0.01 | <0.01 |
| Mg | 12 | 77.0 | 41.0 | 88.0 | 249 | 10.0 | 7.00 |
| Mn | <0.03 | 2.29 | 3.18 | <0.03 | 15.0 | <0.03 | 0.14 |
| Na | 6 | 314.0 | 180 | 28.0 | 1066 | 3.0 | 13.0 |
| P | <0.01 | 0.02 | 0.13 | <0.01 | 0.03 | 0.03 | 0.08 |
| Si | 3.7 | 15.0 | 28.0 | 3.7 | 43.0 | 1.40 | 12.0 |
| Sr | 0.07 | 0.07 | 0.05 | 0.44 | 0.07 | 0.04 | 0.03 |
| Zn | 0.01 | 0.32 | 0.15 | <0.01 | 0.62 | 0.03 | 0.04 |
| Cl | 45.0 | 458 | 231 | 91.0 | 1556 | 10.0 | 4.00 |
| Alkalinity | 66.44 | – | – | – | – | 77.94 | 152.8 |
| F ⁻ | 0.50 | 0.30 | 0.60 | 0.40 | <0.20 | <0.20 | <0.20 |
| NO ₃ ⁻ | 1.40 | 1.60 | 2.00 | 4.30 | 1.20 | 2.60 | 2.10 |
| SO ₄ ²⁻ | 230 | 2191 | 877 | 1912 | 2803 | 13 | 4.00 |

Modelling of the AMD environment was done using PHREEQC with the WATEQ4F database (Parkhurst & Appelo 2013) in order to determine the mineral equilibria (table 4). Because gypsum precipitates were found in the field, it was relevant to predict possible Fe, Ca, Mg and SO_4^{2-} -precipitates. Results show that iron, calcium and sulfate existed bound to the CaCO_3 , CaSO_4 , $\text{CaSO}_4 \cdot 2\text{H}_2\text{O}$ and FeCO_3 phases. Gypsum and anhydrite saturation indices are not too far away from saturation, which explains the gypsum crusts observed in the field.

Table 4 Saturation indices (SI) from water analysis of the Whitehill formation. The SIs close to saturation were selected.

| Mineral Phase | LF1a | LF1b | LF2a | LF2b | CV | LB1 | LB2 |
|--|-------|-------|-------|-------|-------|-------|-------|
| Adularia (KAlSi_3O_8) | -0.62 | – | – | – | – | -4.82 | 0.48 |
| Aragonite (CaCO_3) | -0.58 | – | – | – | – | -1.97 | 0.07 |
| Anhydrite (CaSO_4) | -1.36 | -0.19 | -0.78 | -0.20 | -0.78 | -3.00 | – |
| Calcite (CaCO_3) | -0.44 | – | – | – | – | -1.83 | 0.22 |
| Chalcedony (SiO_2) | -0.66 | -0.04 | 0.22 | -0.65 | 0.22 | -1.08 | -0.15 |
| Cristobalite (SiO_2) | -0.62 | -0.01 | 0.26 | -0.62 | 0.26 | -1.05 | -0.12 |
| Gypsum ($\text{CaSO}_4 \cdot 2\text{H}_2\text{O}$) | -1.14 | 0.02 | -0.56 | 0.02 | -0.56 | -2.80 | -3.13 |
| Jurbanite (AlOH_2SO_4) | – | 0.25 | -0.26 | -1.53 | -0.26 | -4.05 | -7.11 |
| Quartz (SiO_2) | -0.23 | 0.39 | 0.62 | -0.22 | 0.65 | -0.65 | 0.28 |
| Silicagel (SiO_2) | -1.19 | -0.58 | -0.31 | -1.19 | -0.31 | -1.61 | -0.69 |

Conclusions

The Whitehill Formation and its similar strata are results of natural processes occurring in South Africa and worldwide. Evaluation of the Whitehill Formation was conducted in order to predict the mineral equilibria when pyrite bearing shale reacts with calcite. Using PHREEQC modelling (WATE4QF database), it was shown that Fe, Ca and SO_4 formed secondary carbonates and sulfate minerals. In the Witwatersrand Basin, if the discharge of acidic mine water would be prevented, contact of the dolomitic karst aquifer with acidic mine waters would be promoted. As a result, AMD migration can be prevented as suggested by the precipitation of secondary minerals. Thus, it can be concluded that the study of a natural analogue is relevant to understand whether gypsum of the Whitehill Formation is connected to ARD. Furthermore, the Whitehill Formation can be used in future for prevention of AMD issues in the Witwatersrand Basin.

Acknowledgements

We thank the National Research Foundation (NRF) under the SARChI program for funding this project.

References

- Branch T, Ritter O, Weckmann U, Sachsenhofer RF, Schilling F (2007) The Whitehill Formation: a high conductivity marker horizon in the Karoo Basin. *S Afr J Geol* 110(2–3):465–476, doi:10.2113/gssajg.110.2-3.465
- Bruno J, Duro L, Grivé M (2002) The applicability and limitations of thermodynamic geochemical models to simulate trace element behaviour in natural waters: Lessons learned from natural analogue studies. *Chem Geol* 190(1–4):371–393, doi:10.1016/S0009-2541(02)00126-2
- Cole DI, Basson WA (1991) Whitehill Formation. In: Johnson MR, Anhaeusser CR, Thomas RJ (Eds), 2006 *The Geology of South Africa*, Geological society of South Africa: Council for Geoscience, p 51–53
- Durand J (2012) The impact of gold mining of the Witwatersrand on the rivers and karst system of Gauteng and North West Province, South Africa. *J Afr Earth Sci* 68:24–43, doi:10.1016/j.jafrearsci.2012.03.013
- Geel L, De Wit M, Booth P, Schulz HM, Horsfield B (2015) Palaeo-Environment, diagenesis and characteristics of permian black shales in the lower Karoo Supergroup flanking the cape fold belt near Jansenville, Eastern Cape, South Africa: Implications for the shale gas potential of the Karoo Basin. *S Afr J Geol* 118(3):249–274, doi:10.2113/gssajg.118.3.249
- Lottermoser B (2010) *Mine Wastes – Characterization, Treatment and Environmental Impacts*, 3rd edn. Springer, Heidelberg
- Masindi V, Gitari MW, Tutu H, De Beer M (2016) Fate of inorganic contaminants post treatment of acid mine drainage by cryptocrystalline magnesite: Complimenting experimental results with a geochemical model. *J Environ Chem Eng*, 4(4):4846–4856, doi:10.1016/j.jece.2016.03.020
- McCarthy TS (2006) The Witwatersrand Supergroup. In: Johnson MR, Anhaeusser CR, Thomas RJ (Eds), 2006 *The Geology of South Africa*, Geological society of South Africa: Council for Geoscience, p 155–156
- McCarthy TS (2011) The impact of acid mine drainage in South Africa. *J Afr Earth Sci* 107(5/6):712–718, doi:10.4102/sajs.v107i5/6.712
- Nordstrom DK (1982) Aqueous pyrite oxidation and the consequent formation of secondary iron minerals. In: Kittrick JA, Fanning DS, Hossner LR (Eds). *Acid sulfate weathering*. *Soil Sci Soc Am Pub* 37–56.
- Parkhurst DL, Appelo CAJ (2013) Description of Input and Examples for PHREEQC Version 3 – A Computer Program for Speciation, Batch-Reaction, One-Dimensional Transport, and Inverse Geochemical Calculations. *US Geol Surv Tech Methods* 6(A43):1–497
- Smithard T, Borden EM, Reid D (2015) The effect of dolerite intrusions on the hydrocarbon potential of the lower Permian Whitehill formation (Karoo Supergroup) in South Africa and Southern Namibia: A preliminary study. *S Afr J Geol* 118(4):489–510, doi:10.2113/gssajg.118.4.489
- Stewart JH, Poole FG, Wilson RF (1972) Stratigraphy and origin of the Triassic Moenkopi Formation and related strata in the Colorado Plateau region. United States Government Printing Office: Washington, 15-77 pp
- Stumm W, Morgan JJ (1996) *Aquatic chemistry – Chemical Equilibria and Rates in Natural Waters*, 3rd edn. Wiley & Sons, New York
- Wolkersdorfer C (2008) *Water Management at Abandoned Flooded Underground Mines – Fundamentals, Tracer Tests, Modelling, Water Treatment*. Heidelberg, Springer, 222 pp
- Younger PL, Wolkersdorfer C (2004) *Mining Impacts on the Fresh Water Environment: Technical and Managerial Guidelines for Catchment Scale Management*. *Mine Water and the Environment* (2004) 23: S2–S80